Advanced Physical Research
Vol.4, No.1, 2022, pp.33-55

PRODUCTION OF THE VECTOR Z^0-BOSON AND TWO HIGGS BOSONS IN THE POLARIZED ELECTRON-POSITRON COLLISIONS

S.K. Abdullayev*, M.Sh. Gojayev

Baku State University, Baku, Azerbaijan

Abstract. Within the framework of the Standard Model, taking into account the arbitrary polarization states of the electron-positron pair, the differential cross section of the process of associated production of the Higgs boson pair and the vector Z^0-boson is calculated: $e^-e^+ \to HHZ^0$. All Feynman diagrams with the vertex of three Higgs boson (HHH), two Higgs and two Z^0-boson ($HHZZ$), as well as with the vertex of two Z^0- and one Higgs boson (ZZH) interactions are taken into account. Left-right (A_{LR}) and transverse (A_φ) spin asymmetries are determined. The characteristic features of the behavior of the polarization characteristics and the differential effective cross section of the reaction depending on the departure angles and particle energies are investigated and revealed. It is revealed that the left-right spin asymmetry A_{LR} depends only on the Weinberg parameter $sin^2\theta_W$, while the transverse spin asymmetry A_φ is a function of this parameter, the departure angles θ, φ and the energies x_Z, x_1 of particles. The results of calculations of transverse spin asymmetry and differential effective cross section are illustrated by graphs. The possibility of measuring the triple Higgs boson interaction constant g_{HHH} and the interaction constant of two Higgs and two Z bosons g_{ZZHH} is discussed.

Keywords: *electron-positron pair, Higgs boson pair, Standard model, left-right spin asymmetry, transverse spin asymmetry.*

PACS: 13.66.Fg, 14.70.Hp, 14.80.Bn.

Corresponding Author: *S.K. Abdullayev, Baku State University, AZ 1148, Z. Khalilov, 23, Baku, Azerbaijan, Tel.: +994505376210, e-mail: m_qocayev@mail.ru*

Received: *12 January 2022;* ***Accepted:*** *3 March 2022;* ***Published:*** *20 April 2022.*

1. Introduction

The Standard Model (SM) (Glashow, 1967; Weinberg, 1967; Salam, 1968), based on the local gauge symmetry $SU_C(3) \times SU_L(2) \times U_Y(1)$, satisfactorily describes high energy physics (Djouadi, 2005; Abdullayev, 2017; Abdullayev, 2018). The SM introduces a doublet of scalar fields $\varphi = \begin{pmatrix} \varphi^+ \\ \varphi^0 \end{pmatrix}$, the neutral component of which has a vacuum value other than zero. As a result of spontaneous symmetry breaking due to quantum excitations of the scalar field, the Higgs boson H appears, and due to interaction with this field, the gauge bosons $W^\pm$ and Z^0, charged leptons and quarks acquire mass. This mechanism of particle mass generation is known as the mechanism of spontaneous violation of the Brouth-Englert-Higgs symmetry (Higgs, 1964a, 1964b; Englert & Brout, 1964).

The discovery of the Higgs boson H, carried out at the Large Hadron Collider (LHC) by ATLAS and CMS collaborations in 2012 at CERN (ATLAS Collaboration, 2012; CMS Collaboration, 2012) (see also reviews (Rubakov, 2012; Lanyov, 2014; Kazakov, 2014)). With the discovery of the Higgs boson H, the missing particle in SM was found, and this began a new period in the study of the properties of fundamental interactions. In this regard, theoretical and experimental interest in various channels of the production and decay of the Higgs boson H has greatly increased (Barger *et al*., 2003; Abdullayev *et al*., 2015; Abdullayev & Gojayev, 2017; ATLAS Collaboration, 2018; Abdullayev *et al*., 2019; Demirci, 2019; CMS Collaboration, 2021; Abdullayev & Omarova, 2021; Abdullayev & Gojayev, 2022; Kachanovich *et al*., 2022).

The Higgs boson H interacts especially with vector $W^{\pm}$- and Z^0-bosons, because of this, the main sources of the production of Higgs bosons are the radiation of their Z^0- and W-bosons born in various experiments. A particularly intense source of H-bosons could be the processes occurring in electron-positron collisions. It should be noted that the processes occurring during electron-positron annihilation are an effective method for studying the mechanisms of interaction of elementary particles. This is due to the following two circumstances. *Firstly*, the interaction of the e^-e^+-pair is described in SM, so the results obtained are well interpreted. *Secondly*, since the e^-e^+-pair does not participate in strong interactions, the background conditions of experiments are significantly improved compared to the studies conducted in the LHC with proton-proton beams. High-energy electron-positron colliders have already been designed, or are planned to be designed in various laboratories around the world (Shiltsev, 2012; Peters, 2017).

The process of the production of one Higgs boson H in electron-positron collisions $e^-e^+ \to HZ^0$ is considered in a number of papers (Kilian *et al.*, 1996; Djouadi, 2005; Abada, 2013; Greco *et al*., 2016; Gong *et al*., 2017; Greco *et al*., 2018). Here we investigate the process of generation of the Higgs boson of a pair and a vector Z^0-boson in arbitrarily polarized electron-positron collisions

$$e^- + e^+ \to H + H + Z^0. \tag{1}$$

In the case of an unpolarized e^-e^+-pair, this process is considered in the works (Djouadi *et al*., 1999; Barger *et al*., 2003; Djouadi, 2005).

Within the framework of the SM and taking into account arbitrary polarizations of the e^-e^+-pair, an analytical expression for the differential effective cross section of the reaction (1) is obtained. Left-right and transverse spin asymmetries due to the polarizations of the e^-e^+-pair are determined. The dependence of the asymmetries and the effective cross-section of the reaction on the departure angles and particle energies is studied in detail. The possibility of measuring the interaction constant of two Z^0- and two Higgs bosons g_{ZZHH}, and the triple Higgs boson interaction constant g_{HHH} is discussed.

2. Calculation of diagrams a) and b)

The process of the production of the Higgs boson of a pair of HH and a vector Z^0-boson is described by four Feynman diagrams shown in Fig. 1 (4-momentum and spin vectors of particles are indicated in parentheses). First, consider diagram a) with the vertex of the triple Higgs boson interaction. The amplitude of this diagram can be written as follows:

$$M_a = g_{Zee} g_{ZZH} g_{HHH} D_{\mu\nu}(p) D_H(q) \ell_\mu U_\nu^*(k). \tag{2}$$

Here ℓ_μ is a weak neutral electron-positron current:

$$\ell_\mu = \bar{\upsilon}(p_2, s_2)\gamma_\mu[g_L(1+\gamma_5) + g_R(1-\gamma_5)]u(p_1, s_1); \tag{3}$$

g_{Zee} is the constant of the interaction of the Z^0-boson with the e^-e^+-pair; g_{ZZH} and

g_{HHH} are constants of the Z^0- and Higgs boson, triple Higgs boson interactions; according to SM, these constants are equal (Djouadi, 2005):

$$g_{Zee} = (\sqrt{2}G_F)^{1/2}M_Z,\ g_{ZZH} = 2(\sqrt{2}G_F)^{1/2}M_Z^2,\ g_{HHH} = 3(\sqrt{2}G_F)^{1/2}M_H^2,$$

M_Z and M_H are the masses of Z^0- and H-bosons; G_F is the Fermi constant of weak interactions; the left g_L and right g_R electron interaction constants are uniquely determined by the Weinberg parameter $x_W = sin^2\theta_W$:

$$g_L = -\frac{1}{2} + x_W,\ g_R = x_W;$$

s_1 and s_2 are the 4-polarization vectors of the electron and positron, $D_{\mu\nu}(p)$ and $D_H(q)$ are the propagators of the vector Z^0- and scalar H-bosons

$$D_{\mu\nu}(p) = i\frac{-g_{\mu\nu} + p_\mu p_\nu/M_Z^2}{p^2 - M_Z^2},\ D_H(q) = \frac{i}{q^2 - M_H^2};$$

$p = p_1 + p_2$ and $q = k_1 + k_2$ are the total 4-momentus of the electron-positron and Higgs boson pairs; $U_\nu^*(k)$ –is the 4-polarization vector of the Z^0-boson.

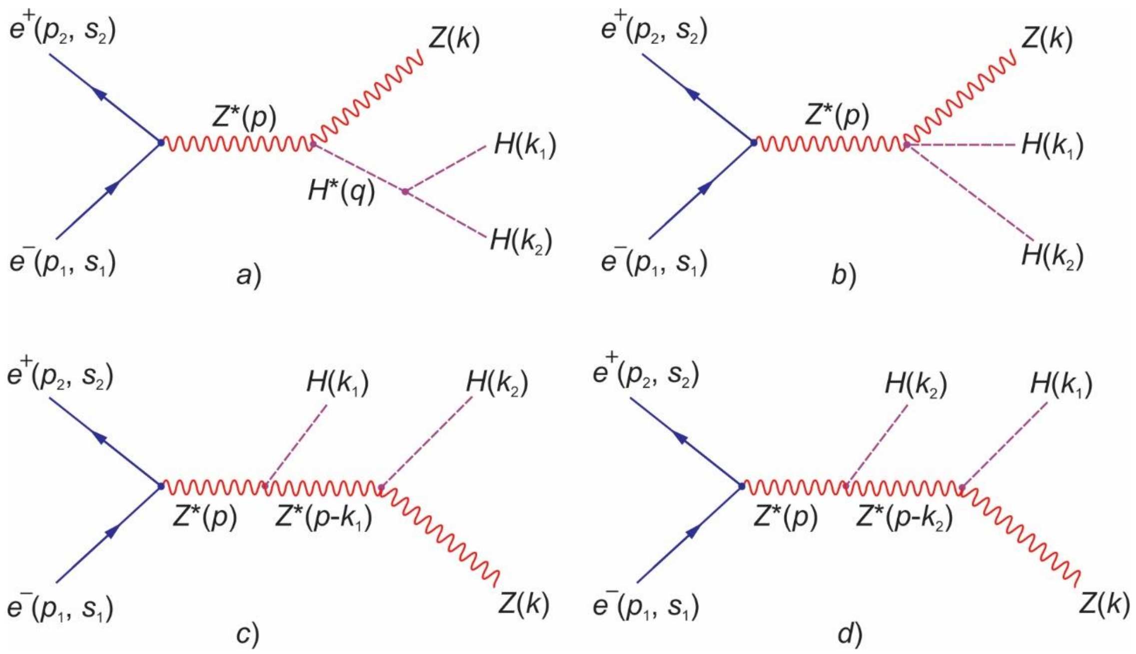

Fig. 1. Feynman diagrams of reaction $e^-e^+ \to ZHH$

At high energies of e^-e^+-pairs $\sqrt{s} >> m$ (where $\sqrt{s}$ is the total energy of e^-e^+-pairs in the center of mass system, m is the mass of electron), a weak neutral electron current is preserved:

$$p_\mu \ell_\mu = (p_1 + p_2)_\mu \ell_\mu = 0,$$

for this reason, the amplitude (2) is simplified

$$M_a = g_{Zee}g_{ZZH}g_{HHH}D_Z(s)D_H(s_1)\ell_\mu U_\mu^*(k), \quad (4)$$

where

$$D_Z(s) = \frac{1}{s(1-r_Z)}, D_H(s_1) = \frac{1}{s_1 - M_H^2} = \frac{1}{s(y_Z + r_Z - r_H)},$$

$s_1 = (k_1 + k_2)^2 = s(1 - x_Z + r_Z)$ is the square of the invariant mass of the Higgs boson pair and the following values are introduced

$$r_Z = \frac{M_Z^2}{s},\ r_H = \frac{M_H^2}{s},\ x_Z = \frac{2E_Z}{\sqrt{s}},\ y_Z = 1 - x_Z. \quad (5)$$

For the modulus of the square of the amplitude (4), the expression was obtained

$$|M_a|^2 = \frac{72\sqrt{2}G_F^3 M_Z^6}{s^2(1-r_Z)^2} \cdot \frac{M_H^4}{s^2(y_Z + r_Z - r_H)^2} L_{\mu\nu} U_\mu^*(k) U_\nu(k). \quad (6)$$

Here $L_{\mu\nu} = \ell_\mu \bar{\ell}_\nu$ is an e^-e^+-pair tensor having the following form

$$\begin{gathered} L_{\mu\nu} = 2(g_L^2 + g_R^2)[p_{1\mu}p_{2\nu} + p_{2\mu}p_{1\nu} - (p_1 \cdot p_2)g_{\mu\nu} - m^2(s_{1\mu}s_{2\nu} + s_{2\mu}s_{1\nu} - \\ -(s_1 \cdot s_2)g_{\mu\nu})] + 2(g_L^2 - g_R^2)m[p_{1\mu}s_{2\nu} + s_{2\mu}p_{1\nu} - (p_1 \cdot s_2)g_{\mu\nu} - p_{2\mu}s_{1\nu} - \\ -s_{1\mu}p_{2\nu} + (p_1 \cdot s_1)g_{\mu\nu})] + 4g_L g_R[(p_1 \cdot s_2)(s_{1\mu}p_{2\nu} + s_{1\nu}p_{2\mu} - (s_1 \cdot p_2)g_{\mu\nu}) + \\ +(p_2 \cdot s_1)\left(p_{1\mu}s_{2\nu} + p_{1\nu}s_{2\mu}\right) - (p_1 \cdot p_2)\left(s_{1\mu}s_{2\nu} + s_{2\mu}s_{1\nu} - (s_1 \cdot s_2)g_{\mu\nu}\right) - \\ (s_1 \cdot s_2)(p_{1\mu}p_{2\nu} + p_{2\mu}p_{1\nu})]. \quad (7) \end{gathered}$$

We summarize by the polarization states of the vector Z^0-boson

$$\sum_{\text{Pol.}} U_\mu^*(k) U_\nu(k) = -g_{\mu\nu} + \frac{k_\mu k_\nu}{M_Z^2}.$$

We calculate the product of the electron and Z^0-boson tensors

$$\begin{gathered} L_{\mu\nu}\left(-g_{\mu\nu} + \frac{k_\mu k_\nu}{M_Z^2}\right) = 2(g_L^2 + g_R^2) \times \\ \times \left[(p_1 \cdot p_2) - m^2(s_1 \cdot s_2) + \frac{2}{M_Z^2}((p_1 \cdot k)(p_2 \cdot k) - m^2(k \cdot s_1)(k \cdot s_2))\right] + \\ +2(g_L^2 - g_R^2)m\left[(p_1 \cdot s_2) - (p_2 \cdot s_1) + \frac{2}{M_Z^2}((p_1 \cdot k)(k \cdot s_2) - (p_2 \cdot k)(k \cdot s_1))\right] + \\ +4g_L g_R\left[(p_1 \cdot p_2)(s_1 \cdot s_2) - (p_1 \cdot s_2)(p_2 \cdot s_1) + \frac{2}{M_Z^2}((p_1 \cdot k)(p_2 \cdot s_1)(k \cdot s_2) + \right. \\ \left. +(p_2 \cdot k)(p_1 \cdot s_2)(k \cdot s_1) - (p_1 \cdot p_2)(k \cdot s_1)(k \cdot s_2) - (p_1 \cdot k)(p_2 \cdot k)(s_1 \cdot s_2))\right]. \quad (8) \end{gathered}$$

The differential effective cross section of the process $e^-e^+ \to HHZ^0$ is related to the square of the amplitude $|M_a|^2$ by the ratio:

$$\begin{gathered} \frac{d^3\sigma_a}{dx_Z dx_1 d\Omega} = \frac{1}{64} \cdot \frac{|M_a|^2}{(2\pi)^4} = \\ = \frac{9\sqrt{2}G_F^3 M_Z^6}{128\pi^4 s^2(1-r_Z)^2} \cdot \frac{r_H^2}{(y_Z + r_Z - r_H)^2} L_{\mu\nu}\left(-g_{\mu\nu} + \frac{k_\mu k_\nu}{M_Z^2}\right), \quad (9) \end{gathered}$$

where the product of the electron-positron and Z^0-boson tensors is given by expression (8), $d\Omega = \sin\theta\, d\theta d\varphi$ is the solid angle of departure of the Z^0-boson, θ is the angle between the directions of the electron and Z^0-boson momentums.

Let us consider some special cases of the differential effective cross section (9). First, assume that the e^-e^+-pair is longitudinally polarized:

$$s_{1\mu} = \frac{\sqrt{s}}{2m}\lambda_1(1,\vec{n}),\ s_{2\mu} = \frac{\sqrt{s}}{2m}\lambda_2(1,-\vec{n}).$$

Here λ_1 and λ_2 are the helicities of the electron and positron, $\vec{n}$ is a unit vector in the direction of the electron momentum.

In this case, the differential effective cross section (9) will take the form

$$\frac{d^3\sigma_a(\lambda_1,\lambda_2)}{dx_Z dx_1 d\Omega} = \frac{9\sqrt{2}}{512\pi^4}\cdot\frac{G_F^3M_Z^6}{s(1-r_Z)^2}\cdot\frac{r_H^2}{(y_Z+r_Z-r_H)^2}\cdot\frac{1}{r_Z}\times$$
$$\times\,[g_L^2(1-\lambda_1)(1+\lambda_2)+g_R^2(1+\lambda_1)(1-\lambda_2)][x_Z^2\sin^2\theta+4r_Z(1+\cos^2\theta)]. \quad (10)$$

From this effective cross-section formula it follows that the electron and positron must have opposite helicities: $\lambda_1=-\lambda_2=\pm1$ (electron left, positron right – $e_L^-e_R^+$ or electron right positron left – $e_R^-e_L^+$). This fact is due to the preservation of the total moment in the transition $e^-+e^+\to Z^0$.

Now consider the case when an electron-positron pair is transversely polarized

$$s_{1\mu}=(0,\vec{\eta}_1),\ s_{2\mu}=(0,\vec{\eta}_2),$$

where $\vec{\eta}_1$ and $\vec{\eta}_2$ are the transverse components of the spin vectors of the electron and positron.

Let's direct the electron's momentum along the Z axis, and its spin vector $\vec{\eta}_1$ along the *X* axis (see Fig. 2), then the spin vector $\vec{\eta}_2$ will lie in the *XOY* plane, the angle between the spin vectors $\vec{\eta}_1$ and $\vec{\eta}_2$ is denoted by Φ. In this case, the differential effective cross section (9) will take the form:

$$\frac{d^3\sigma_a(\vec{\eta}_1,\vec{\eta}_2)}{dx_Z dx_1 d\Omega} = \frac{9\sqrt{2}G_F^3M_Z^6}{512\pi^4 s r_Z}\cdot\frac{1}{(1-r_Z)^2}\cdot\left(\frac{r_H}{y_Z+r_Z-r_H}\right)^2\{(g_L^2+g_R^2)\times$$
$$\times\,[x_Z^2\sin^2\theta+4r_Z(1+\cos^2\theta)]-2g_Lg_R\eta_1\eta_2(x_Z^2-4r_Z)\sin^2\theta\cos(2\varphi-\Phi)\}. \quad (11)$$

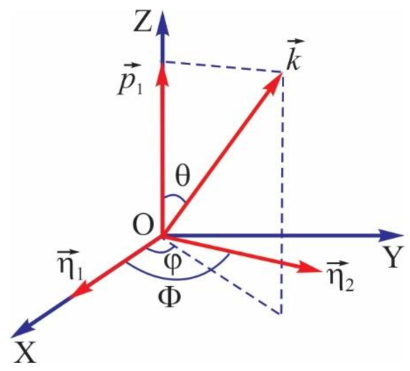

Fig. 2. Choosing a coordinate system

Now we proceed with the calculation of the Feynman diagram b) in Fig. 1 with the vertex of two Z^0- and two H-bosons. The amplitude of this diagram will be written as follows

$$M_b = -ig_{Zee}g_{ZZHH}\ell_\mu D_{\mu\nu}(p)U_\nu^*(k), \quad (12)$$

where g_{ZZHH} is the interaction constant defined in SM by the expression

$$g_{ZZHH} = 2\sqrt{2}G_F M_Z^2.$$

Based on the amplitude (12), the following expression is obtained for the differential effective cross section of the process $e^-e^+ \to HHZ^0$, taking into account arbitrary polarizations of the e^-e^+-pair

$$\frac{d^3\sigma_b(\lambda_1,\lambda_2,\eta_1,\eta_2)}{dx_Z dx_1 d\Omega} = \frac{\sqrt{2}G_F^3 M_Z^6}{512\pi^4 s(1-r_Z)^2}\cdot\frac{1}{r_Z}\times$$
$$\times\{[g_L^2(1-\lambda_1)(1+\lambda_2)+g_R^2(1+\lambda_1)(1-\lambda_2)][x_Z^2\sin^2\theta+4r_Z(1+\cos^2\theta)]+$$
$$+2g_L g_R\eta_1\eta_2(x_Z^2-4r_Z^2)\sin^2\theta\cos 2\varphi\}. \quad (13)$$

It should be noted that there is interference between diagrams a) and b). Taking into account the interference of these diagrams for the differential cross section of the reaction (1), the following expression is obtained (e^-e^+-the pair is arbitrarily polarized, the angle Φ is assumed to be π):

$$\frac{d^3\sigma_{a+b}}{dx_Z dx_1 d\Omega} = \frac{\sqrt{2}G_F^3 M_Z^6}{512\pi^4 s(1-r_Z)^2}\cdot\frac{1}{r_Z}\left(1-\frac{3r_H}{y_Z+r_Z-r_H}\right)^2\times$$
$$\times\{[g_L^2(1-\lambda_1)(1+\lambda_2)+g_R^2(1+\lambda_1)(1-\lambda_2)][x_Z^2\sin^2\theta+4r_Z(1+\cos^2\theta)]+$$
$$+2g_L g_R\eta_1\eta_2(x_Z^2-4r_Z^2)\sin^2\theta\cos 2\varphi\}. \quad (14)$$

Based on the effective cross-section formula (14), we determine the left-right spin asymmetry due to the longitudinal polarization of an electron or positron:

$$A_{LR} = \frac{g_L^2-g_R^2}{g_L^2+g_R^2} = \frac{0.25-x_W}{0.25-x_W+2x_W^2}. \quad (15)$$

The left-right spin asymmetry A_{LR} depends only on the Weinberg parameter x_W and with the value of this parameter $x_W = 0{,}2315$ is $A_{LR} = 14\%$.

It also follows from the expression of the effective cross section (14) that an azimuthal angular asymmetry should be observed in the angular distribution of the Z^0-boson, determined by the formula

$$A_\varphi = \frac{2g_L g_R}{g_L^2+g_R^2}\cdot\frac{(x_Z^2-4r_Z)\sin^2\theta}{x_Z^2\sin^2\theta+4r_Z(1+\cos^2\theta)}\cdot\cos 2\varphi. \quad (16)$$

Azimuthal asymmetry A_φ is sometimes called transverse spin asymmetry, since it occurs only during annihilation of a transversely polarized e^-e^+-pair. The transverse spin asymmetry A_φ is maximal at the azimuthal departure angle $\varphi = 0$ and π, it depends on both the polar angle θ and the energy x_Z.

Figure 3 shows the angular dependence of the transverse spin asymmetry A_φ at $\sqrt{s}$ =500 GeV, $M_Z = 91.1875$ GeV, $x_W = 0.2315$ and various Z-boson energies: 1) $x_Z = 0.4$; 2) $x_Z = 0.6$; 3) $x_Z = 0.78$. As follows from the figure, the transverse spin asymmetry A_φ is negative, with an increase in the angle of departure θ it decreases and reaches a minimum at an angle $\theta = 90°$. Further growth of the angle θ leads to an increase in the transverse spin asymmetry. With an increase in the fraction of energy x_Z carried away by the Z^0-boson, the graph of the dependence of the transverse spin asymmetry A_φ on the angle θ is located below.

Fig. 4 illustrates the energy dependence of the transverse spin asymmetry A_φ at different departure angles of the Z^0-boson: 1) $\theta = 30°$; 2) $\theta = 60°$; 3) $\theta = 90°$. It can be seen from the figure that with an increase in the energy of the Z^0-boson, the transverse spin asymmetry decreases, an increase in the angle θ also leads to a decrease in the transverse spin asymmetry A_{φ}.

Averaging the cross section (14) over the polarization states of the $e^{-}e^{+}$-pair and integrating over the departure angles of the Z^{0}-boson, we obtain the energy spectrum of the particles:

$$\frac{d^{2}\sigma_{a+b}}{dx_{Z}dx_{1}}=\frac{G_{F}^{3}M_{Z}^{6}}{96\sqrt{2}\pi^{3}}\cdot\frac{x_{Z}^{2}+8r_{Z}}{sr_{Z}(1-r_{Z})^{2}}\left(1-\frac{3r_{H}}{y_{Z}+r_{Z}-r_{H}}\right)^{2}(g_{L}^{2}+g_{R}^{2}). \tag{17}$$

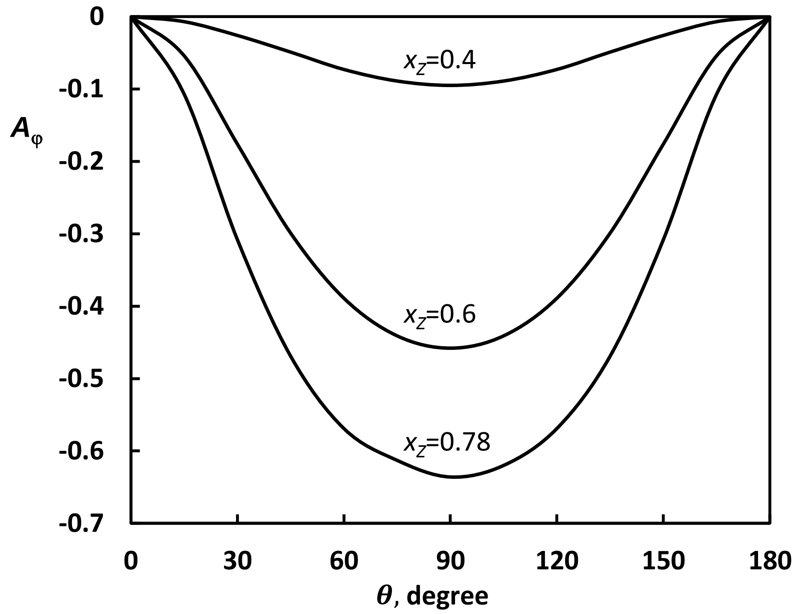

Fig. 3. Angular dependence of the asymmetry A_{φ} at different energies x_{Z}

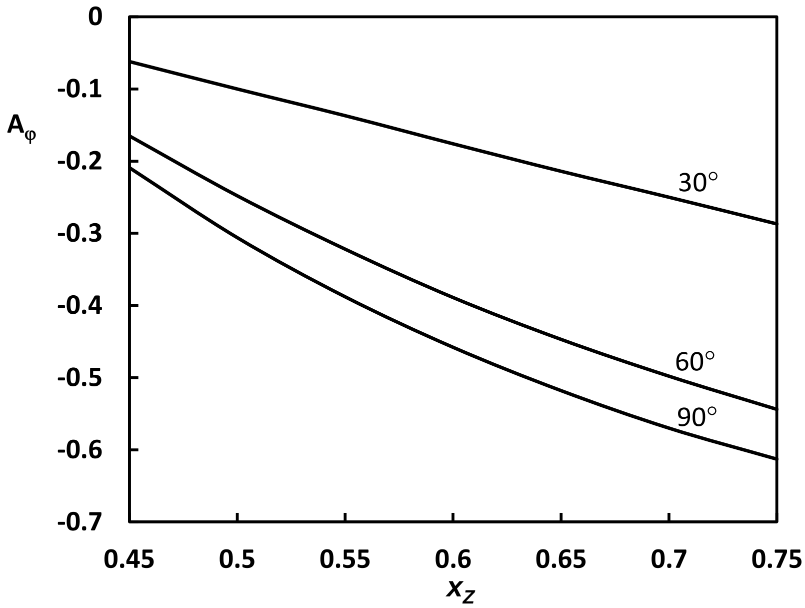

Fig. 4. Energy dependence of asymmetry A_{φ} at different angles θ

Figure 5 shows the energy dependence of the cross section reaction $e^{-}e^{+}\to HHZ^{0}$ on the variable x_{Z} at the energy $e^{-}e^{+}$-pair $\sqrt{s}$=500 GeV. It follows from the figure that with an increase in the fraction of energy carried away by the Z^{0}-boson, the cross section monotonically decreases.

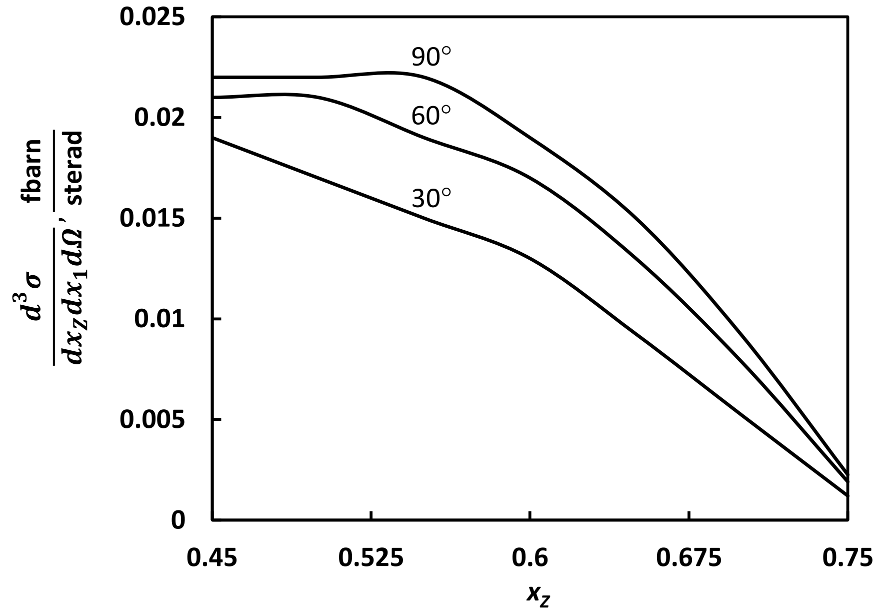

Fig. 5. Dependence of the cross section reaction $e^-e^+ \to ZHH$ on the energy x_Z

3. Calculation of diagrams c) and d)

The amplitude corresponding to diagram c) Fig. 1 can be written as:

$$M_c = g_{Zee} g_{ZZH}^2 \ell_\mu D_{\mu\nu}(p) D_{\nu\rho}(q) U_\rho^*(k), \tag{18}$$

where $q = p - k_1 = k_1 + k_2$.

As noted above, at high energies, the weak neutral current of the e^-e^+-pair is preserved, as a result, the amplitude is simplified:

$$M_c = g_{Zee} g_{ZZH}^2 \cdot \frac{1}{s(1 - r_Z)} \cdot \frac{1}{s(y_1 + r_H - r_Z)} \cdot \ell_\mu \cdot \left(g_{\mu\rho} - \frac{q_\mu q_\rho}{M_Z^2} \right) U_\rho^*(k), \tag{19}$$

where $y_1 = 1 - x_1$, $x_1 = 2E_1/\sqrt{s}$, E_1 is the Higgs boson energy with 4-momentum k_1.

For the modulus of the square of the matrix element (19), the expression is obtained:

$$|M_c|^2 = \frac{g_{Zee}^2}{s^2(1 - r_Z)^2} \frac{g_{ZZH}^4}{s^2(y_1 + r_H - r_Z)^2} \times$$

$$\times L_{\mu\nu} \left(g_{\mu\rho} - \frac{q_\mu q_\rho}{M_Z^2} \right) \cdot \left(g_{\nu\sigma} - \frac{q_\nu q_\rho}{M_Z^2} \right) \cdot \left(-g_{\rho\sigma} + \frac{k_\rho k_\sigma}{M_Z^2} \right). \tag{20}$$

Here $L_{\mu\nu} = \ell_\mu \bar{\ell}_\nu$ is the electron-positron tensor (7). In (20), the tensor

$$\sum_{\text{pol.}} U_\rho^*(k) U_\sigma(k) = -g_{\rho\sigma} + \frac{k_\rho k_\sigma}{M_Z^2}$$

arises due to the summation of the vector Z^0-boson over the polarization states.

We define the product of the electron-positron $L_{\mu\nu}$ and Z^0-boson tensors

$$L_{\mu\nu} \left(-g_{\rho\sigma} + \frac{k_\rho k_\sigma}{M_Z^2} \right) \left(g_{\mu\rho} - \frac{q_\mu q_\rho}{M_Z^2} \right) \cdot \left(g_{\nu\sigma} - \frac{q_\nu q_\sigma}{M_Z^2} \right) = L_{\mu\nu} \times$$

$$\times\left[-g_{\mu\nu}+\frac{k_\mu k_\nu}{M_Z^2}+\frac{k_{1\mu}k_{1\nu}}{M_Z^2}\left(2-\frac{y_1+r_H}{r_Z}+\frac{(y_1+r_Z)^2}{4r_Z^2}\right)+\frac{k_\mu k_{1\nu}+k_\nu k_{1\mu}}{M_Z^2}\cdot\frac{y_1+r_Z}{2r_Z}\right]=$$

$$=2(g_L^2+g_R^2)\left[(p_1\cdot p_2)-m^2(s_1\cdot s_2)+\frac{2}{M_Z^2}((p_1\cdot k)(p_2\cdot k)-m^2(k\cdot s_1)(k\cdot s_2))\right]+$$

$$+2(g_L^2-g_R^2)m\left[(p_1\cdot s_2)-(p_2\cdot s_1)+\frac{2}{M_Z^2}\big((p_1\cdot k)(k\cdot s_2)-(p_2\cdot k)(k\cdot s_1)\big)\right]+4g_Lg_R\times$$

$$\times\Big[(p_1\cdot p_2)(s_1\cdot s_2)-(p_1\cdot s_2)(p_2\cdot s_1)+\frac{2}{M_Z^2}\ ((p_1\cdot s_2)(k\cdot s_1)(k\cdot p_2)+$$

$$+(p_2\cdot s_1)(k\cdot s_2)(k\cdot p_1)-(p_1\cdot p_2)(k\cdot s_1)(k\cdot s_2)-(s_1\cdot s_2)(p_1\cdot k)(p_2\cdot k)\Big]+$$

$$+\left(2-\frac{y_1+r_H}{r_Z}+\frac{(y_1+r_Z)^2}{4r_Z^2}\right)\cdot\frac{2}{M_Z^2}\{(g_L^2+g_R^2)[2(p_1\cdot k_1)(p_2\cdot k_1)-M_H^2(p_1\cdot p_2)-$$

$$-m^2(2(k_1\cdot s_1)(k_1\cdot s_2)-M_H^2(s_1\cdot s_2))]+(g_L^2-g_R^2)m[2(k_1\cdot p_1)(k_1\cdot s_2)-$$

$$-M_H^2(p_1\cdot s_2)-2(k_1\cdot p_2)(k_1\cdot s_1)+M_H^2(p_2\cdot s_1))]+2g_Lg_R[(p_1\cdot s_2)(2(k_1\cdot p_2)(k_1\cdot s_1)-$$

$$-M_H^2(p_2\cdot s_1))-(p_1\cdot p_2)(2(k_1\cdot s_1)(k_1\cdot s_2)-M_H^2(s_1\cdot s_2))+2(p_2\cdot s_1)(k_1\cdot p_1)\times$$

$$\times(k_1\cdot s_2)-2(s_1\cdot s_2)(p_1\cdot k_1)(p_2\cdot k_1)]\}+$$

$$+\frac{y_1+r_Z}{r_Z}\frac{2}{M_Z^2}\{(g_L^2+g_R^2)[(k\cdot p_1)(k_1\cdot p_2)+(k\cdot p_2)(k_1\cdot p_1)-(p_1\cdot p_2)(k\cdot k_1)-$$

$$-m^2((k\cdot s_1)(k_1\cdot s_2)+(k\cdot s_2)(k_1\cdot s_1)-(s_1\cdot s_2)(k\cdot k_1)]+(g_L^2-g_R^2)m[(k\cdot p_1)\times$$

$$\times(k_1\cdot s_2)+(k\cdot s_2)(k_1\cdot p_1)-(p_1\cdot s_2)(k\cdot k_1)-(k\cdot s_1)(k_1\cdot p_2)-(k\cdot p_2)(k_1\cdot s_1)+$$

$$+(p_2\cdot s_1)(k\cdot k_1)]+2g_Lg_R[(p_1\cdot s_2)((k\cdot s_1)(k_1\cdot p_2)+(k\cdot p_2)(k_1\cdot s_1)-$$

$$-(p_1\cdot s_2)(k\cdot k_1))-(p_1\cdot p_2)((k\cdot s_1)(k_1\cdot s_2)+(k\cdot s_2)(k_1\cdot s_1)-(s_1\cdot s_2)(k\cdot k_1))+$$

$$+(p_2\cdot s_1)((k\cdot p_1)(k_1\cdot s_2)+(k\cdot s_2)(k_1\cdot p_1))-(s_1\cdot s_2)\times$$

$$\times((k\cdot p_1)(k_1\cdot p_2)+(k\cdot p_2)(k_1\cdot p_1))]\}. \qquad (21)$$

The differential effective cross section of the reaction $e^-e^+\to HHZ^0$ is expressed by the formula

$$\frac{d^3\sigma_c}{dx_Zdx_1d\Omega}=\frac{1}{64}\cdot\frac{|M_c|^2}{(2\pi)^4}=\frac{\sqrt{2}G_F^3M_Z^6}{32\pi^4s^2(1-r_Z)^2}\cdot\frac{r_Z^2}{(y_1+r_H-r_Z)^2}L_{\mu\nu}\times$$

$$\times\left[-g_{\mu\nu}+\frac{k_\mu k_\nu}{M_Z^2}+\frac{k_{1\mu}k_{1\nu}}{M_Z^2}\left(2-\frac{y_1+r_H}{r_Z}+\frac{(y_1+r_Z)^2}{4r_Z^2}\right)+\frac{k_\mu k_{1\nu}+k_\nu k_{1\mu}}{M_Z^2}\cdot\frac{y_1+r_Z}{2r_Z}\right], \qquad (22)$$

where the product of the electron-positron $L_{\mu\nu}$ and Z^0-boson tensors is given by expression (21). In the system center-of-mass e^-e^+-a pair for $\vec{p}_1+\vec{p}_2=\vec{k}+\vec{k}_1+\vec{k}_2=0$ end particles lie in the same plane with the azimuthal angle φ of departure.

In the system of the center of mass e^-e^+-pairs, the laws of conservation of energy and momentum in the variables x_Z, x_1, x_2 and angles θ, θ_1, θ_2 are written as follows:

$$x_Z+x_1+x_2=2,$$

$$\sqrt{x_Z^2-4r_Z}\,cos\,\theta+\sqrt{x_1^2-4r_H}\,cos\,\theta_1+\sqrt{x_2^2-4r_H}\,cos\,\theta_2=0.$$

Here θ_1 (θ_2) is the angle between the directions of the electron momentums and the first (second) Higgs boson. The energy of the Z^0-boson is enclosed in the region

$$\frac{2M_Z}{\sqrt{s}} \leq x_Z \leq 1 + r_Z - 4r_H.$$

Let us consider special cases of differential effective cross-section (22). If the e^-e^+-pair is longitudinally polarized, then the effective cross section (22) will take the form

$$\frac{d^3\sigma_c(\lambda_1,\lambda_2)}{dx_Z dx_1 d\Omega} = \frac{\sqrt{2}G_F^3 M_Z^6}{128\pi^4 s(1-r_Z)^2} \cdot \frac{r_Z}{(y_1 + r_H - r_Z)^2} \times$$
$$\times [g_L^2(1-\lambda_1)(1+\lambda_2) + g_R^2(1+\lambda_1)(1-\lambda_2)] \times$$
$$\times \left\{ x_Z^2 \sin^2\theta + 4r_Z(1+\cos^2\theta) + \left(2 - \frac{y_1 + r_H}{r_Z} + \frac{(y_1+r_Z)^2}{4r_Z^2}\right)(x_1^2 - 4r_H)\sin^2\theta_1 + \right.$$
$$\left. + \frac{y_1 + r_Z}{r_Z}\left[x_Z x_1 - \sqrt{(x_Z^2 - 4r_Z)(x_1^2 - 4r_H)}\cos\theta\cos\theta_1 - 2(y_2 - z_Z)\right] \right\}, \qquad (23)$$

where $y_2 = 1 - x_2$.

It follows from the formula of the differential effective cross section (23) that the cross section of the process $e_L^- e^+ \to HHZ^0$ differs from the cross section of the reaction $e_R^- e^+ \to HHZ^0$. Therefore, the process under consideration $e^-e^+ \to HHZ^0$ has a left-right spin asymmetry

$$A_{LR} = \frac{g_L^2 - g_R^2}{g_L^2 + g_R^2}.$$

As noted above, with the value of the parameter x_W =0,2315, the left-right (or longitudinal) spin asymmetry is $A_{LR} = 14\%$.

If the electron and positron are transversely polarized, then the differential effective cross section is expressed by the formula

$$\frac{d^3\sigma_c(\eta_1,\eta_2)}{dx_Z dx_1 d\Omega} = \frac{\sqrt{2}}{128\pi^4} \cdot \frac{G_F^3 M_Z^6}{s(1-r_Z)^2} \cdot \frac{r_Z}{(y_1 + r_H - r_Z)^2} \times$$
$$\times [(g_L^2 + g_R^2)f_1 + 2g_L g_R \eta_1 \eta_2 f_2]. \qquad (24)$$

Here

$$f_1 = x_Z^2 \sin^2\theta + 4r_Z(1+\cos^2\theta) + \left(2 - \frac{y_1 + r_H}{r_Z} + \frac{(y_1+r_Z)^2}{4r_Z^2}\right)(x_1^2 - 4r_H)\sin^2\theta_1 +$$
$$+ \frac{y_1 + r_Z}{r_Z}\left[x_Z x_1 - \sqrt{(x_Z^2 - 4r_Z)(x_1^2 - 4r_H)}\cos\theta\cos\theta_1 - 2(y_2 - z_Z)\right], \qquad (25)$$

$$f_2 = -(x_Z^2 - 4r_Z)\sin^2\theta\cos(2\varphi - \Phi) - \left(2 - \frac{y_1 + r_H}{r_Z} + \frac{(y_1+r_Z)^2}{4r_Z^2}\right) \times$$
$$\times (x_1^2 - 4r_H)\sin^2\theta_1\cos(2\varphi - \Phi) + \frac{y_1 + r_Z}{r_Z} \times$$
$$\times \left[\cos\Phi\left(x_Z x_1 - \sqrt{(x_Z^2 - 4r_Z)(x_1^2 - 4r_H)}\cos\theta\cos\theta_1 - \sqrt{(x_Z^2 - 4r_Z)(x_1^2 - 4r_H)} \times\right.\right.$$

$$\times \sin\theta \sin\theta_1 \left(\cos\Phi + \cos(2\varphi - \Phi)\right) - 2(y_2 - r_Z)\cos\Phi\Big]. \qquad (26)$$

It can be seen from the formula of the differential effective cross section (24) that the process $e^- e^+ \to HHZ^0$ has a transverse spin asymmetry determined by the formula (the angle Φ between the vectors $\vec{\eta}_1$ and $\vec{\eta}_2$ is assumed to be π)

$$A_\varphi(\theta,\varphi) = \frac{2g_L g_R}{g_L^2 + g_R^2} \cdot \frac{f_2}{f_1}, \qquad (27)$$

in this case , the function f_2 is equal to

$$f_2 = (x_Z^2 - 4r_Z)\sin^2\theta\cos 2\varphi + \left(2 - \frac{y_1 + r_H}{r_Z} + \frac{(y_1 + r_Z)^2}{4r_Z^2}\right)(x_1^2 - 4r_H) \times$$
$$\times \sin^2\theta_1 \cos 2\varphi + \frac{y_1 + r_Z}{r_Z}\Big[-x_Z x_1 + \sqrt{(x_Z^2 - 4r_Z)(x_1^2 - 4r_H)} \times$$
$$\times (\cos\theta\cos\theta_1 + \sin\theta\sin\theta_1(1 + \cos 2\varphi) + 2(y_2 - r_Z)\Big]. \qquad (28)$$

Figure 6 shows the angular dependence of the transverse spin asymmetry $A_\varphi(\theta,\varphi)$ at $\varphi = 0$, $\sqrt{s}$ =500 GeV, $x_1 = 0.5$ and various values of the Z^0-boson energy: 1) x_Z =0.4; 2) x_Z =0.45; 3) x_Z =0.5. As can be seen from the figure, the transverse spin asymmetry is positive, with the increase in the angle θ decreases and reaches a minimum at an angle of θ =90°, and with further increase in the angle θ asymmetry $A_\varphi(\theta,\varphi)$ begins to grow. An increase in the energy x_Z leads to a decrease in asymmetry.

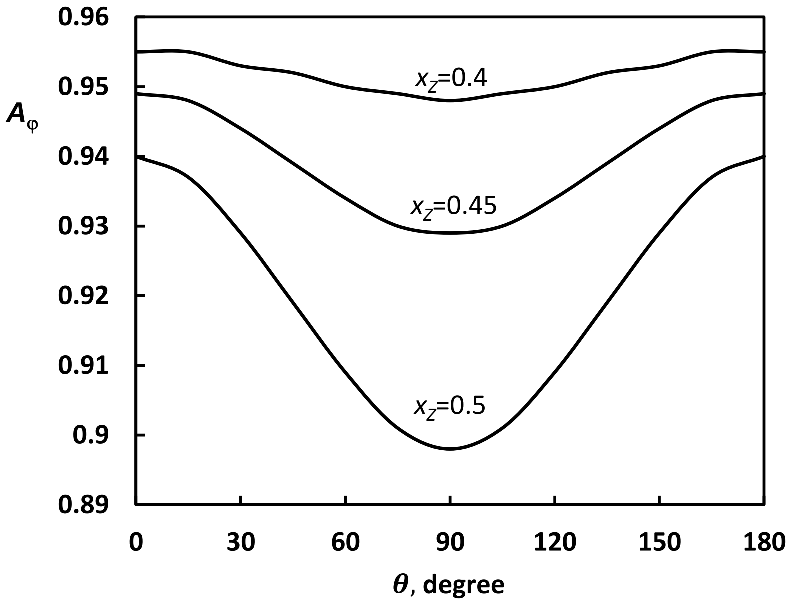

Fig. 6. Dependence of the asymmetry $A_\varphi(\theta,\varphi = 0)$ on the angle θ at different energies x_Z

Fig. 7 illustrates the dependence of transverse-spin asymmetry from the azimuthal angle φ in $x_Z = x_1 = 0.5$ and different values of the polar emission angle θ: 1) $\theta = 30°$; 2) $\theta = 60°$; 3) $\theta = 90°$. As follows from the figure, the transverse spin asymmetry is positive, with an increase in the azimuth angle φ it increases and reaches a maximum at $\theta = 90°$, and then with an increase in the angle φ, the transverse spin asymmetry decreases and reaches a minimum at $\theta = 180°$. With further increase of the azimuthal angle φ from 180° to 360° graphs of the dependence of the asymmetry $A_\varphi(\theta, \varphi)$ of φ angle again. With an increase in the polar angle, the transverse spin asymmetry at the points of maximum ($\varphi = 90°$; 270) almost does not change, and at the points of minimum $\varphi = 0°; 180°; 360°$) decreases.

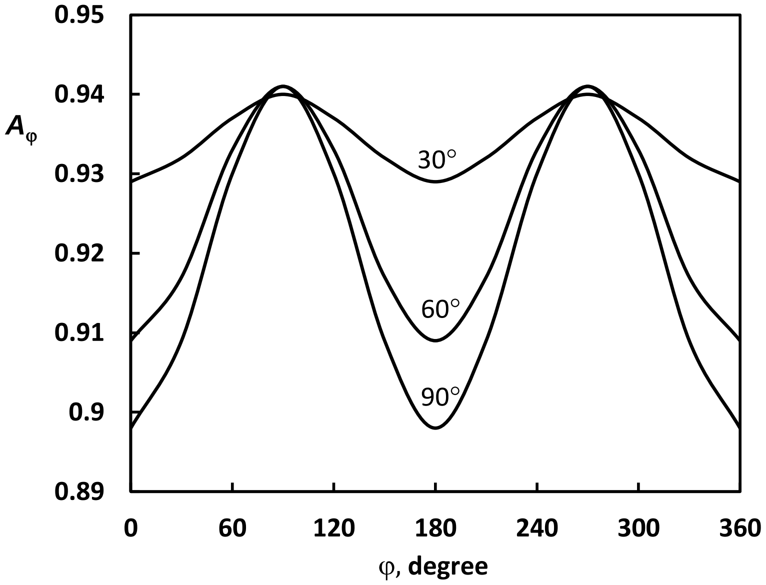

Fig. 7. Dependence of the transverse spin asymmetry on the azimuthal angle φ at different angles θ.

Fig. 8 shows the dependence of the transverse-spin asymmetry of the energy x_Z at $\sqrt{s}$ =500 GeV, $\varphi = 0$, $x_1 = 0.5$ and various angles θ: 1) $\theta = 30°$; 2) $\theta = 60°$; 3) $\theta = 90°$. With an increase in the fraction of energy x_Z, carried away by the Z^0-boson, the transverse spin asymmetry monotonically decreases, and an increase in the polar angle θ also leads to a decrease in asymmetry.

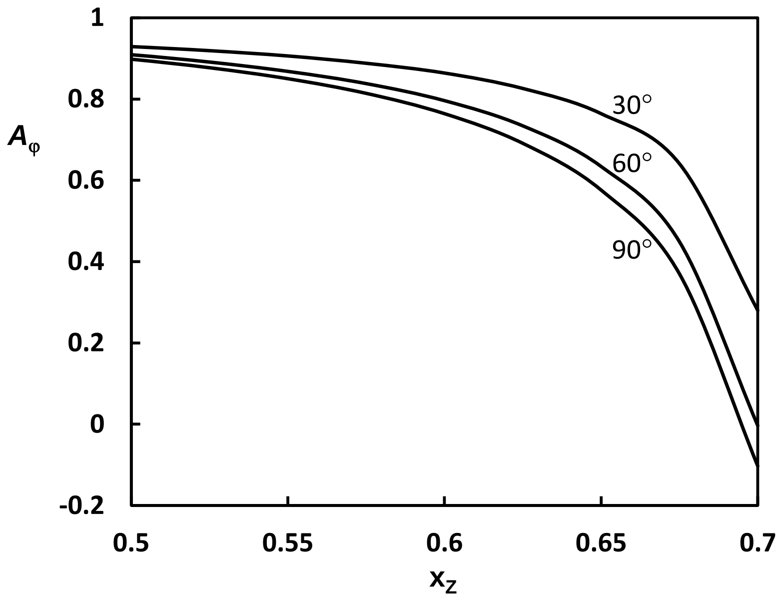

Fig. 8. Dependence of the transverse spin asymmetry on the energy x_Z at $\varphi = 0$, $x_1 = 0.5$ and various departure angles θ

We now proceed with the calculation of diagram d) Fig. 1, the amplitude of which can be written as follows:

$$M_d = g_{Zee} g_{ZZH}^2 \frac{1}{s(1-r_Z)} \frac{1}{s(y_2+r_H-r_Z)} \ell_\mu \left(g_{\mu\rho} - \frac{q'_\mu q'_\rho}{M_Z^2} \right) U_\rho^*(k), \qquad (29)$$

where $q'_\mu = (p-k_2)_\mu = (k+k_1)_\mu$ is the total 4-momentum of Z^0- and Higgs bosons. Based on this amplitude, the following expression was obtained for the differential effective cross section of the reaction $e^-e^+ \to HHZ^0$ (the e^-e^+-pair is arbitrarily polarized):

$$\frac{d^3\sigma_d(\lambda_1,\lambda_2,\eta_1,\eta_2)}{dx_Z dx_1 d\Omega} = \frac{\sqrt{2} G_F^3 M_Z^6}{128\pi^4 s(1-r_Z)^2} \cdot \frac{r_Z}{(y_2+r_H-r_Z)^2} \times$$
$$\times \{[(g_L^2(1-\lambda_1)(1+\lambda_2) + g_R^2(1+\lambda_1)(1-\lambda_2)] \cdot F_1 + 2g_L g_R \eta_1 \eta_2 F_2]\}. \qquad (30)$$

Here the functions F_1 and F_2 are obtained from the functions f_1 and f_2 (they are given by formulas (25) and (26)) by substitutions

$$\theta_1 \to \theta_2, x_1 \to x_2, y_1 \to y_2.$$

Consider the interference of diagrams c) and d) Fig. 1

$$M_c^+ M_d + M_d^+ M_c = 2\frac{g_{Zee}^2}{s^2(1-r_Z)^2} \frac{g_{ZZH}^4}{s^2(y_1+r_H-r_Z)(y_2+r_H-r_Z)} \times$$
$$\times L_{\mu\nu} \left[-g_{\mu\nu} + \frac{k_\mu k_\nu}{M_Z^2} + \frac{k_{1\mu} k_{1\nu}}{M_Z^2} + \frac{k_{2\mu} k_{2\nu}}{M_Z^2} - \frac{k_\mu k_{1\nu} + k_{1\mu} k_\nu}{2M_Z^2} \frac{y_2 - r_Z}{2r_Z} - \right.$$
$$\left. - \frac{k_\mu k_{2\nu} + k_{2\mu} k_\nu}{2M_Z^2} \frac{y_1 - r_Z}{2r_Z} - \frac{k_{1\mu} k_{2\nu} + k_{2\mu} k_{1\nu}}{2M_Z^2} \frac{1}{2r_Z} \left(y_Z + r_Z - 2r_H - \frac{y_1 - r_Z}{2r_Z}(y_2 - r_Z) \right) \right] =$$
$$= 2\frac{g_{Zee}^2}{s^2(1-r_Z)^2} \cdot \frac{g_{ZZH}^4}{s^2(y_1+r_H-r_Z)} \cdot \frac{2}{(y_2+r_H-r_Z)} \times$$
$$\times \left\{ (g_L^2 + g_R^2) \left[(p_1 \cdot p_2) - m^2(s_1 \cdot s_2) + \frac{2}{M_Z^2}((p_1 \cdot k)(p_2 \cdot k) - m^2(k \cdot s_1)(k \cdot s_2)) \right] + \right.$$
$$+ (g_L^2 - g_R^2) m \cdot \left[(p_1 \cdot s_2) - (p_2 \cdot s_1) + \frac{2}{M_Z^2}((p_1 \cdot k)(k \cdot s_2) - (p_2 \cdot k)(k \cdot s_1)) \right] +$$
$$+ 2g_L g_R \left[(p_1 \cdot p_2)(s_1 \cdot s_2) - (p_1 \cdot s_2)(p_2 \cdot s_1) + \frac{2}{M_Z^2}((p_1 \cdot s_2)(k \cdot s_1)(p_2 \cdot k) + \right.$$
$$\left. + (p_2 \cdot s_1)(k \cdot s_2)(p_1 \cdot k) - (p_1 \cdot p_2)(k \cdot s_1)(k \cdot s_2) - (s_1 \cdot s_2)(p_1 \cdot k)(p_2 \cdot k)) \right] +$$
$$+ \frac{1}{M_Z^2} [(g_L^2 + g_R^2)(2(p_1 \cdot k_1)(p_2 \cdot k_1) - M_H^2(p_1 \cdot p_2) - m^2(2(k_1 \cdot s_1)(k_1 \cdot s_2) -$$
$$- M_H^2(s_1 \cdot s_2))) + (g_L^2 - g_R^2) m \cdot (2(p_1 \cdot k_1)(k_1 \cdot s_2) - M_H^2(p_1 \cdot s_2) -$$
$$- 2(p_2 \cdot k_1)(k_1 \cdot s_1) + M_H^2(p_2 \cdot s_1)) + 2g_L g_R((p_1 \cdot s_2)(2(k_1 \cdot s_1)(p_2 \cdot k_1) -$$
$$- M_H^2(p_2 \cdot s_1)) + 2(p_2 \cdot s_1)(p_1 \cdot k_1)(k_1 \cdot s_2) - (p_1 \cdot p_2)(2(k_1 \cdot s_1)(k_1 \cdot s_2) -$$
$$- M_H^2(s_1 \cdot s_2)) - 2(s_1 \cdot s_2)(p_1 \cdot k_1)(p_2 \cdot k_1)) + (k_1 \to k_2)] +$$

$$+\frac{y_2-r_Z}{2r_Z}\cdot\frac{1}{M_Z^2}[(g_L^2+g_R^2)((p_1\cdot k)(p_2\cdot k_1)+(p_1\cdot k_1)(p_2\cdot k)-(p_1\cdot p_2)(k\cdot k_1)-$$
$$-m^2((k\cdot s_1)(k_1\cdot s_2)+(k_1\cdot s_1)(k\cdot s_2)-(s_1\cdot s_2)(k\cdot k_1)))+$$
$$+(g_L^2-g_R^2)m((p_1\cdot k)(k\cdot s_2)+(p_1\cdot k_1)(k\cdot s_2)-(p_1\cdot s_2)(k\cdot k_1)-$$
$$-(k\cdot s_1)(p_2\cdot k_1)-(p_2\cdot k)(k\cdot s_1)+(p_2\cdot s_1)(k\cdot k_1))+$$
$$+2g_Lg_R((p_1\cdot s_2)((k\cdot s_1)(p_2\cdot k_1)+(k_1\cdot s_1)(k\cdot p_2)-(p_2\cdot s_1)(k\cdot k_1))-$$
$$-(p_2\cdot s_1)((p_1\cdot k)(k_1\cdot s_2)+(p_1\cdot k_1)(k\cdot s_2))-(p_1\cdot p_2)((k\cdot s_1)(k_1\cdot s_2)+$$
$$+(k\cdot s_2)(k_1\cdot s_1)-(s_1\cdot s_2)(k\cdot k_1))-(s_1\cdot s_2)((p_1\cdot k)(p_2\cdot k_1)+$$
$$+(p_2\cdot k)(p_1\cdot k_1)))]-\frac{y_1-r_Z}{2r_Z}\cdot\frac{1}{M_Z^2}[k_1\to k_2]-$$
$$-\frac{1}{2r_Z}\left(y_Z+r_Z-2r_H-\frac{(y_1-r_Z)(y_2-r_Z)}{r_Z}\right)\cdot\frac{1}{M_Z^2}\cdot[(g_L^2+g_R^2)((p_1\cdot k_1)(p_2\cdot k_2)+$$
$$+(p_1\cdot k_2)(p_2\cdot k_1)-(p_1\cdot p_2)(k_1\cdot k_2)-m^2((k_1\cdot s_1)(k_2\cdot s_3)+(k_1\cdot s_2)(k_2\cdot s_1)-$$
$$-(s_1\cdot s_2)(k_1\cdot k_2)))+(g_L^2-g_R^2)m((p_1\cdot k_1)(k_2\cdot s_2)-(p_1\cdot k_2)(k_1\cdot s_2)-$$
$$-(p_1\cdot s_2)(k_1\cdot k_2)-(k_1\cdot s_1)(k_2\cdot p_2)-(k_2\cdot s_1)(k_1\cdot p_2)+(p_2\cdot s_1)(k_1\cdot k_2))+$$
$$+2g_Lg_R((p_1\cdot s_2)((k_1\cdot s_1)(k_2\cdot p_2)+(k_2\cdot s_1)(k_1\cdot p_2)-(p_2\cdot s_1)(k_1\cdot k_2)+$$
$$+(p_2\cdot s_1)((k_1\cdot p_1)(k_2\cdot s_2)+(k_2\cdot p_1)(k_1\cdot s_2))-(p_1\cdot p_2)((k_1\cdot s_1)(k_2\cdot s_2)+$$
$$+(k_1\cdot s_2)(k_2\cdot s_1)-(s_1\cdot s_2)(k_1\cdot k_2))-(s_1\cdot s_2)((p_1\cdot k_1)(p_2\cdot k_2)+$$
$$+(p_1\cdot k_2)(p_2\cdot k_1)))]\}. \tag{31}$$

Here the sign $k_1\to k_2$ means that this expression is obtained from the previous expression by replacing the 4-momentum k_1 with k_2.

Then, based on this matrix element for the contribution to the cross section of the process $e^-e^+\to HHZ^0$ interference diagrams c) and d), we obtain the expression (angle Φ accepted π)

$$\frac{d^3\sigma_{c,d}^{(\text{inter.})}}{dx_Zdx_1d\Omega}=\frac{\sqrt{2}}{64\pi^4}\cdot\frac{G_F^3M_Z^6}{s(1-r_Z)^2}\cdot\frac{r_Z}{(y_1+r_H-r_Z)(y_2+r_H-r_Z)}\times$$
$$\times\Big\{g_L^2(1-\lambda_1)(1+\lambda_2)+g_R^2(1+\lambda_1)(1-\lambda_2)]\Big[x_Z^2\sin^2\theta+4r_Z(1+\cos^2\theta)+$$
$$+\left(x_1^2-4r_H\right)\sin^2\theta_1+(x_2^2-4r_H)\sin^2\theta_2-$$
$$-\frac{y_2-r_Z}{2r_Z}\left(x_Zx_1-\sqrt{(x_Z^2-4r_Z)(x_1^2-4r_H)}\cdot\cos\theta\cos\theta_1-2(y_2-r_Z)\right)-$$
$$-\frac{y_1-r_Z}{2r_Z}\left(x_Zx_2-\sqrt{(x_Z^2-4r_Z)(x_2^2-4r_H)}\cdot\cos\theta\cos\theta_2-2(y_1-r_Z)\right)-$$
$$-\frac{1}{2r_Z}(x_1x_2-\sqrt{(x_1^2-4r_H)(x_2^2-4r_H)}\cdot\cos\theta_1\cos\theta_2-2(y_Z+r_Z-2r_H)\times$$
$$\times\left(y_Z+r_Z-2r_H-\frac{1}{2r_Z}(y_1-r_Z)(y_2-r_Z)\right)\Big]+2g_Lg_R\eta_1\eta_2\Big[\Big((x_Z^2-4r_Z)\sin^2\theta+$$

$$+(x_1^2-4r_H)\,sin^2\theta_1-(x_2^2-4r_H)\,sin^2\theta_2\Big)cos\,2\varphi+$$
$$+\frac{y_2-r_Z}{2r_Z}\left(x_Zx_1-\sqrt{(x_Z^2-4r_Z)(x_1^2-4r_H)}\,cos(\theta-\theta_1)-2(y_2-r_Z)\right)-$$
$$-\sqrt{(x_Z^2-4r_Z)(x_1^2-4r_H)}\cdot sin\,\theta\, sin\,\theta_1\, cos(2\varphi)+$$
$$+\frac{y_1-r_Z}{2r_Z}\left(x_Zx_2-\sqrt{(x_Z^2-4r_Z)(x_2^2-4r_H)}\cdot cos(\theta-\theta_2)-2(y_1-r_Z)\right)-$$
$$-\sqrt{(x_Z^2-4r_Z)(x_2^2-4r_H)}\,cos(\theta_1-\theta_2)-2(y_Z+r_Z-2r_H)-$$
$$-\sqrt{(x_1^2-4r_H)(x_2^2-4r_H)}\cdot sin\,\theta_1\, sin\,\theta_2\, cos(2\varphi))\Big]\Big\}. \qquad (32)$$

Figure 9 shows the angular dependence of the differential effective cross section of the process $e^-e^+\to HHZ^0$ at $\sqrt{s}$ =500 GeV, x_1 =0.5, x_W =0.2315 and various energy values of the Z^0-boson x_Z: 1) x_Z =0.5; 2) x_Z =0.6; 3) x_Z =0.7. As follows from the figure, with an increase in the angle θ, the differential effective cross section increases and reaches a maximum at $\theta=90°$, a further increase in the angle leads to a decline in the effective cross section. An increase in the fraction of energy x_Z carried away by the Z^0 boson leads to a decrease in the differential effective cross section.

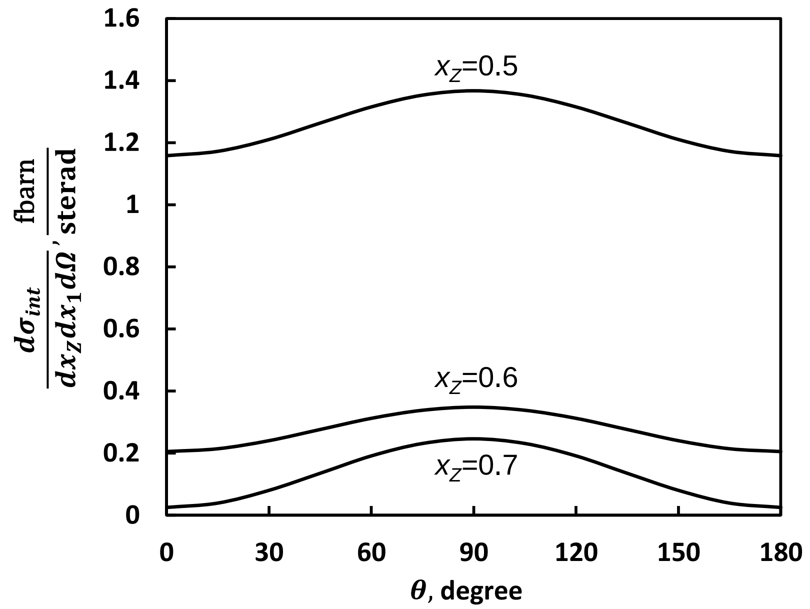

Fig. 9. Angular dependence of the reaction cross section $e^-e^+\to HHZ^0$ at different x_Z

Figure 10 illustrates the dependence of the differential effective cross section on the variable x_Z at $\sqrt{s}$ =500 GeV, x_1 =0.5 and various values of the departure angle θ: 1) $\theta=30°$; 2) $\theta=90°$. As can be seen from the figure, with an increase in the variable x_Z, the effective cross section increases and reaches a maximum at x_Z= 0.475, and a further increase in the energy carried away by the Z^0-boson leads to a decrease in the effective cross section. At the maximum, the effective cross-section reaches the value $d^3\sigma/dx_Zdx_1d\Omega$ =45.75 fbarn/sterad at $\theta=90°$.

4. Interference calculation diagram a), b) and c), d)

In sections 2 and 3, we calculated the differential effective cross sections of the process $e^-e^+ \to HHZ^0$ taking into account the Feynman diagrams a), b) and c), d) Fig. 1. Here we also consider the interference of these diagrams.

During annihilation of an arbitrarily polarized electron-positron pair, the following expressions are obtained for the interference of these diagrams:

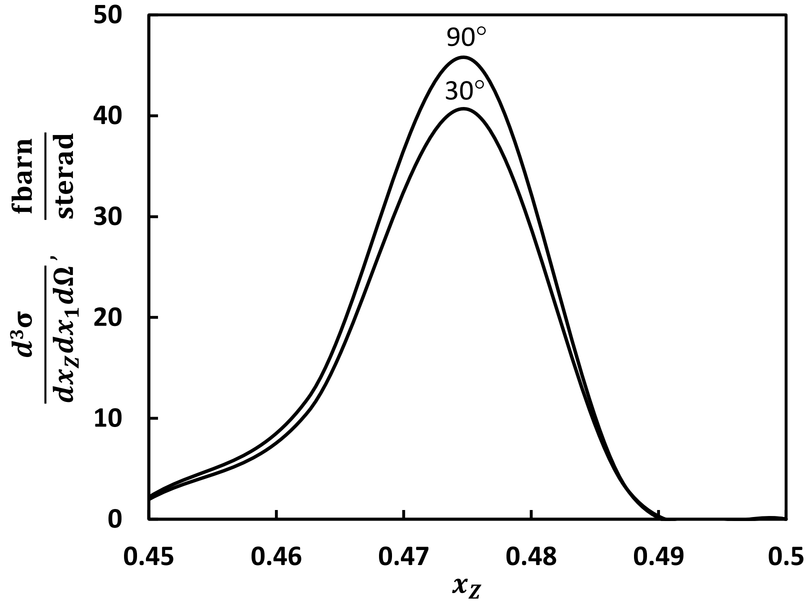

Fig. 10. Energy dependence of the reaction cross section $e^-e^+ \to HHZ^0$ at different θ

$$\frac{d^3\sigma_{a,c}^{(\text{inter.})}}{dx_Z dx_1 d\Omega} = \frac{3\sqrt{2}}{128\pi^4} \cdot \frac{G_F^3 M_Z^6}{s(1-r_Z)^2} \cdot \frac{r_H}{y_Z + r_Z - r_H} \cdot \frac{1}{y_1 + r_H - r_Z} \times$$
$$\times \{-[g_L^2(1-\lambda_1)(1+\lambda_2) + g_R^2(1+\lambda_1)(1-\lambda_2)][x_Z^2 \sin^2\theta + 4r_Z(1+\cos^2\theta) +$$
$$+(x_1^2 - 4r_H)\sin^2\theta_1 + \frac{y_1 + r_Z}{2r_Z} \cdot (x_Z x_1 - \sqrt{(x_Z^2 - 4r_Z)(x_1^2 - 4r_H)}\cos\theta\cos\theta_1 -$$
$$-2(y_2 - r_Z))] + 2g_L g_R \eta_1 \eta_2[-(x_Z^2 - 4r_Z)\sin^2\theta\cos(2\varphi) -$$
$$-(x_1^2 - 4r_H)\sin^2\theta_1\cos(2\varphi) + \frac{y_1 + r_Z}{2r_Z}(x_Z x_1 - \sqrt{(x_Z^2 - 4r_Z)(x_1^2 - 4r_H)}\cos(\theta - \theta_1) -$$
$$-2(y_2 - r_Z) - \sqrt{(x_Z^2 - 4r_Z)(x_1^2 - 4r_H)}\sin\theta\sin\theta_1\cos(2\varphi))]\}; \quad (33)$$

$$\frac{d^3\sigma_{a,d}^{(\text{inter.})}}{dx_Z dx_1 d\Omega} = \frac{3\sqrt{2}}{128\pi^4} \cdot \frac{G_F^3 M_Z^6}{s(1-r_Z)^2} \cdot \frac{r_H}{y_Z + r_Z - r_H} \cdot \frac{1}{y_2 + r_H - r_Z} \times$$
$$\times \{-[g_L^2(1-\lambda_1)(1+\lambda_2) + g_R^2(1+\lambda_1)(1-\lambda_2)][x_Z^2 \sin^2\theta + 4r_Z(1+\cos^2\theta) +$$
$$+(x_2^2 - 4r_H)\sin^2\theta_2 + \frac{y_2 + r_Z}{2r_Z} \cdot (x_Z x_2 - \sqrt{(x_Z^2 - 4r_Z)(x_2^2 - 4r_H)}\cos\theta\cos\theta_2 -$$
$$-2(y_1 - r_Z))] + 2g_L g_R \eta_1 \eta_2[-((x_Z^2 - 4r_Z)\sin^2\theta\cos(2\varphi) -$$

$$-(x_2^2-4r_H)\,sin^2\theta_2)\,cos(2\varphi)+\frac{y_2+r_Z}{2r_Z}(x_Zx_2-\sqrt{(x_Z^2-4r_Z)(x_2^2-4r_H)}\,cos(\theta-\theta_2)-$$

$$-2(y_1-r_Z))-\sqrt{(x_Z^2-4r_Z)(x_2^2-4r_H)}\,sin\,\theta\,sin\,\theta_2\,cos(2\varphi))]\}; \qquad (34)$$

$$\frac{d^3\sigma_{b,c}^{(\text{inter})}}{dx_Zdx_1d\Omega}=\frac{\sqrt{2}G_F^3M_Z^6}{256\pi^4}\cdot\frac{1}{s(1-r_Z)^2}\cdot\frac{1}{y_1+r_H-r_Z}\cdot\frac{r_H}{r_Z}\times$$

$$\times\{-[g_L^2(1-\lambda_1)(1+\lambda_2)+g_R^2(1+\lambda_1)(1-\lambda_2)][x_Z^2\,sin^2\theta+4r_Z(1+cos^2\theta)+$$

$$+(x_1^2-4r_H)\,sin^2\theta_1+\frac{y_2+r_Z}{2r_Z}(x_Zx_1-\sqrt{(x_Z^2-4r_Z)(x_1^2-4r_H)}\,cos\,\theta\,cos\,\theta_1-$$

$$-2(y_2-r_Z))]+2g_Lg_R\eta_1\eta_2[-((x_Z^2-4r_Z)\,sin^2\theta\,cos(2\varphi)-(x_1^2-4r_H)\,sin^2\theta_1)\times$$

$$\times\,cos(2\varphi)+\frac{y_1+r_Z}{2r_Z}(x_Zx_1-\sqrt{(x_Z^2-4r_Z)(x_1^2-4r_H)}\,cos(\theta-\theta_1)-2(y_2-r_Z))-$$

$$-\sqrt{(x_Z^2-4r_Z)(x_1^2-4r_H)}\,sin\,\theta\,sin\,\theta_1\,cos(2\varphi))]\}; \qquad (35)$$

$$\frac{d^3\sigma_{b,d}^{(\text{inter.})}}{dx_Zdx_1d\Omega}=\frac{\sqrt{2}G_F^3M_Z^6}{256\pi^4}\cdot\frac{1}{s(1-r_Z)^2}\cdot\frac{1}{y_2+r_H-r_Z}\cdot\frac{r_H}{r_Z}\times$$

$$\times\{-[g_L^2(1-\lambda_1)(1+\lambda_2)+g_R^2(1+\lambda_2)(1-\lambda_1)][x_Z^2\,sin^2\theta+4r_Z(1+cos^2\theta)+$$

$$+(x_2^2-4r_H)\,sin^2\theta_2+\frac{y_2+r_Z}{2r_Z}\cdot(x_Zx_2-\sqrt{(x_Z^2-4r_Z)(x_2^2-4r_H)}\,cos\,\theta\,cos\,\theta_2-$$

$$-2(y_1-r_Z))]+2g_Lg_R\eta_1\eta_2[(-(x_Z^2-4r_Z)\,sin^2\theta-(x_2^2-4r_H)\,sin^2\theta_2)\,cos(2\varphi)+$$

$$+\frac{y_2+r_Z}{2r_Z}(x_Zx_2-\sqrt{(x_Z^2-4r_Z)(x_2^2-4r_H)}\,cos(\theta-\theta_2)-2(y_1-r_H))-$$

$$-\sqrt{(x_Z^2-4r_Z)(x_2^2-4r_H)}\,sin\,\theta\,sin\,\theta_2\,cos(2\varphi))]\}. \qquad (36)$$

Thus, we calculated the differential effective cross section of the process $e^-e^+\to HHZ^0$ taking into account all possible Feynman diagrams (Fig. 1, a, b, c, d) and arbitrary polarization states of the electron-positron pair. The differential effective cross section of the process under consideration consists of sections of diagrams a), b) (formula (14)), sections of diagrams c), d) and their interference (formulas (24), (30) and (32)), as well as interference of diagrams a) and c), a) and d), b) and c), b) and d) (formulas (33)-(36)).

We estimate the left-right and transverse spin asymmetries A_{LR} and $A_\varphi(x_Z,\theta)$ taking into account all Feynman diagrams shown in Fig. 1. All formulas of the differential effective cross sections of helicities an electron and a positron are included in the form

$$[g_L^2(1-\lambda_1)(1+\lambda_2)+g_R^2(1+\lambda_1)(1-\lambda_2)],$$

therefore, the left-right or longitudinal spin asymmetry due to the longitudinal polarization of the electron is expressed by the formula

$$A_{LR}=\frac{g_L^2-g_R^2}{g_L^2+g_R^2}.$$

As for the transverse spin asymmetry $A_\varphi(x_Z,\theta)$, we estimate it at $x_1=0.5$ by the formula

$$A_\phi(x_Z,\theta) = \frac{2g_L g_R}{g_L^2+g_R^2}\cdot\frac{\psi_2}{\psi_1}, \tag{37}$$

where functions ψ_1 and ψ_2 are defined as

$$\begin{aligned}
\psi_1 = {} & \frac{1}{4r_Z}\left(1-\frac{3r_H}{y_Z+r_Z-r_H}\right)^2[x_Z^2\sin^2\theta+4r_Z(1+\cos^2\theta)]+\\
&+\frac{r_Z}{(y_1+r_H-r_Z)^2}\cdot[x_Z^2\sin^2\theta+4r_Z(1+\cos^2\theta)+\frac{y_1+r_Z}{r_Z}(x_Zx_1-2(y_2-r_Z))]+\\
&+\frac{r_Z}{(y_2+r_H-r_Z)^2}\cdot\left[x_Z^2\sin^2\theta+4r_Z(1+\cos^2\theta)+\left(2-\frac{y_1+r_H}{r_Z}+\frac{(y_1+r_Z)^2}{4r_Z^2}\right)\times\right.\\
&\times(x_2^2-4r_H)\sin^2\theta_2+\frac{y_2+r_Z}{r_Z}\cdot(x_Zx_2-\sqrt{(x_Z^2-4r_Z)(x_2^2-4r_H)}\cos\theta\cos\theta_2-\\
&\left.-2(y_1-r_Z))\right]+\frac{2}{y_1+r_H-r_Z}\cdot\frac{r_Z}{(y_2+r_H-r_Z)}\cdot\left[x_Z^2\sin^2\theta+4r_Z(1+\cos^2\theta)+\right.\\
&+(x_2^2-4r_H)\sin^2\theta_2-\frac{y_2-r_Z}{2r_Z}(x_Zx_1-2(y_2-r_Z))-\frac{y_1-r_Z}{2r_Z}\cdot(x_Zx_2-\\
&-\sqrt{(x_Z^2-4r_Z)(x_2^2-4r_H)}\cos\theta\cos\theta_2-2(y_1-r_Z))-\frac{1}{2r_Z}(x_1x_2-2(y_Z+r_Z-2r_H))\times\\
&\left.\times\left(y_Z+r_Z-2r_H-\frac{1}{2r_Z}(y_1-r_Z)(y_2-r_Z)\right)\right]-\frac{3}{y_Z+r_Z-r_H}\cdot\frac{r_H}{y_1+r_H-r_Z}\times\\
&\times\left[x_Z^2\sin^2\theta+4r_Z(1+\cos^2\theta)+\frac{y_1+r_Z}{2r_Z}(x_Zx_1-2(y_2-r_Z))\right]-\\
&-\frac{3}{y_Z+r_Z-r_H}\cdot\frac{r_H}{y_2+r_H-r_Z}\left[x_Z^2\sin^2\theta+4r_Z(1+\cos^2\theta)+(x_2^2-4r_H)\sin^2\theta_2+\right.\\
&\left.+\frac{y_2+r_Z}{2r_Z}(x_Zx_2-\sqrt{(x_Z^2-4r_Z)(x_2^2-4r_H)}\cos\theta\cos\theta_2-2(y_1-r_Z))\right]-\\
&-\frac{r_H}{2r_Z}\cdot\frac{1}{y_1+r_H-r_Z}\left[x_Z^2\sin^2\theta+4r_Z(1+\cos^2\theta)+\frac{y_1+r_Z}{2r_Z}(x_Zx_1-2(y_2-r_H))\right]-\\
&-\frac{r_H}{2r_Z}\cdot\frac{1}{y_2+r_H-r_Z}\left[x_Z^2\sin^2\theta+4r_Z(1+\cos^2\theta)+(x_2^2-4r_H)\sin^2\theta_2+\right.\\
&\left.+\frac{y_2+r_Z}{2r_Z}\cdot(x_Zx_2-\sqrt{(x_Z^2-4r_Z)(x_2^2-4r_H)}\cos\theta\cos\theta_2-2(y_1-r_Z))\right];
\end{aligned} \tag{38}$$

$$\begin{aligned}
\psi_2 = {} & \frac{1}{4r_Z}\left(1-\frac{3r_H}{y_Z+r_Z-r_H}\right)^2[(x_Z^2-4r_Z)\sin^2\theta\cos 2\varphi+\frac{r_Z}{(y_1+r_H-r_Z)^2}\times\\
&\times[(x_Z^2-4r_Z)\sin^2\theta\cos 2\varphi+\frac{y_1+r_Z}{r_Z}(-x_Zx_1+2(y_2-r_Z))]+\frac{r_Z}{(y_2+r_H-r_Z)^2}\times\\
&\times\left[(x_Z^2-4r_Z)\sin^2\theta\cos 2\varphi+\left(2-\frac{y_1+r_H}{r_Z}+\frac{(y_1+r_Z)^2}{4r_Z^2}\right)(x_2^2-4r_H)\sin^2\theta_2\cos 2\varphi+\right.\\
&+\frac{y_2+r_Z}{r_Z}\cdot(-x_Zx_2+\sqrt{(x_Z^2-4r_Z)(x_2^2-4r_H)}(\cos\theta\cos\theta_2+\sin\theta\sin\theta_2\times\\
&\times(1+\cos 2\varphi)+2(y_1-r_Z))]+\frac{2}{y_1+r_H-r_Z}\cdot\frac{r_Z}{y_2+r_H-r_Z}\times
\end{aligned}$$

$$\times\left[cos\,2\,\varphi((x_Z^2 - 4r_Z)\,sin^2\,\theta - (x_2^2 - 4r_H)\,sin^2\,\theta_2) + \frac{y_2 - r_Z}{2r_Z}\times\right.$$
$$\times\,(x_Z x_1 - 2(y_2 - r_Z)) + \frac{y_1 - r_Z}{2r_Z}\cdot(x_Z x_2 - \sqrt{(x_Z^2 - 4r_Z)(x_2^2 - 4r_H)}\,cos(\,\theta - \theta_2) -$$
$$-2(y_1 - r_Z) - \sqrt{(x_Z^2 - 4r_Z)(x_2^2 - 4r_H)}\cdot sin\,\theta\,sin\,\theta_2\,cos\,2\,\varphi) + \frac{1}{2r_Z}\times$$
$$\times\left(y_Z + r_Z - 2r_H - \frac{(y_1 - r_Z)(y_2 - r_Z)}{2r_Z}\right)\cdot(x_1 x_2 - 2(y_Z + r_Z - 2r_H))\Bigg] + \frac{3}{y_Z + r_Z - r_H}\times$$
$$\times\frac{r_H}{y_1 + r_H - r_Z}\cdot\left[-(x_Z^2 - 4r_Z)\,sin^2\,\theta\,cos\,2\varphi + \frac{y_1 + r_Z}{2r_Z}(x_Z x_1 - 2(y_2 - r_Z))\right] +$$
$$+\frac{3}{y_Z + r_Z - r_H}\cdot\frac{r_H}{y_2 + r_Z - r_H}\cdot\Bigg[cos\,2\,\varphi(-(x_Z^2 - 4r_Z)\,sin^2\,\theta - (x_2^2 - 4r_H)\,sin^2\,\theta_2) +$$
$$+\frac{y_2 + r_Z}{2r_Z}(x_Z x_2 - \sqrt{(x_Z^2 - 4r_Z)(x_2^2 - 4r_H)}\,cos(\,\theta - \theta_2) - 2(y_1 - r_Z) -$$
$$-\sqrt{(x_Z^2 - 4r_Z)(x_2^2 - 4r_H)}\cdot sin\,\theta\,sin\,\theta_2\,cos\,2\,\varphi)\Bigg] +$$
$$+\frac{r_H}{2r_Z}\cdot\frac{1}{y_1 + r_H - r_Z}\left[-(x_Z^2 - 4r_Z)\,sin^2\,\theta\,cos\,2\,\phi + \frac{y_1 + r_Z}{2r_Z}(x_Z x_1 - 2(y_2 - r_Z))\right] +$$
$$+\frac{r_H}{2r_Z}\cdot\frac{1}{y_2 + r_H - r_Z}[cos\,2\,\varphi(-(x_Z^2 - 4r_Z)\,sin^2\,\theta - (x_2^2 - 4r_H)\,sin^2\,\theta_2] +$$
$$+\frac{y_2 + r_Z}{2r_Z}(x_Z x_2 - \sqrt{(x_Z^2 - 4r_Z)(x_2^2 - 4r_H)}\,cos(\,\theta - \theta_2) - 2(y_1 - r_H) -$$
$$-\sqrt{(x_Z^2 - 4r_Z)(x_2^2 - 4r_H)}\cdot sin\,\theta\,sin\,\theta_2\,cos\,2\,\varphi)]. \qquad (39)$$

When obtaining the expressions of the functions ψ_1 and ψ_2, it is taken into account that, in the case of $x_1 = 0.5x_1^2 - 4r_H = 0$, and the angle θ_2 between the directions of the electron momentums and the second Higgs boson with 4-momentum k_2 is associated with the angle θ by the ratio

$$cos\,\theta_2 = -\sqrt{\frac{x_Z^2 - 4r_Z}{x_2^2 - 4r_H}}\,cos\,\theta.$$

Figure 11 shows the dependence of the transverse spin asymmetry $A_\varphi(x_Z, \theta)$ on the polar angle θ at different energy values x_Z: 1) $x_Z = 0.55$; 2) x_Z =0.60; 3) x_Z =0.65. As can be seen from the figure, the transverse spin asymmetry is positive and at x_Z =0.55 and x_Z =0.60 with an increase in the angle θ it decreases and reaches a minimum at an angle $\theta = 90°$, and with a further increase in the angle the value of the asymmetry increases. However, at x_Z=0.65, an inverse angular dependence is observed, that with an increase in the angle θ, the transverse spin asymmetry increases and reaches a maximum at θ =90°, and with a further increase in the angle, the asymmetry decreases.

Fig. 12 illustrates the dependence of transverse-spin asymmetry from the proportion of energy x_Z, entrained Z^0-boson at different angles θ: 1) $\theta = 45°$; 2) $\theta = 60°$; 3) $\theta = 90°$. It follows from the figure that with increasing x_Z, the transverse spin asymmetry monotonically decreases.

Averaging over the polarization states of e^-e^+-pairs for the differential effective cross section of the reaction $e^-e^+ \to HHZ^0$ we have the formula (all Feynman diagrams are taken into account)

$$\frac{d^3\sigma}{dx_Z dx_1 d\Omega} = \frac{\sqrt{2}G_F^3 M_Z^6}{128\pi^4 s} \cdot \frac{1}{(1-r_Z)^2} \cdot \psi_1, \tag{40}$$

where the function ψ_1 is given by formula (38).

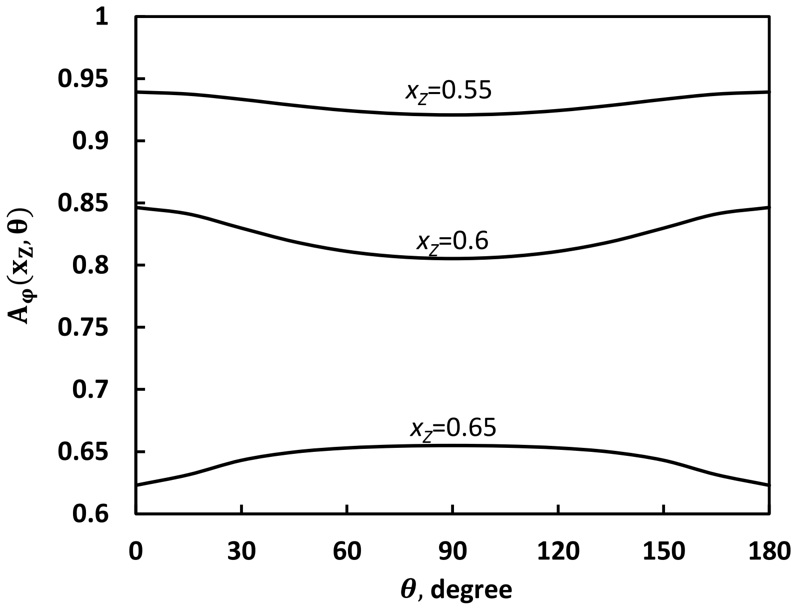

Fig. 11. Angular dependence of the transverse spin asymmetry at different x_Z.

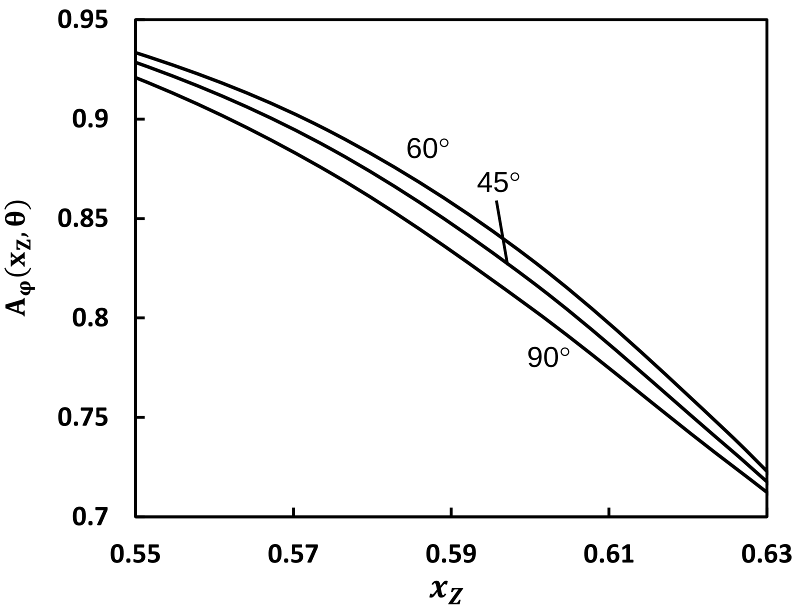

Fig. 12. Energy dependence of transverse spin asymmetry at different angles θ

Figure 13 shows the angular dependence of the differential effective cross section of the reaction $e^-e^+ \to HHZ^0$ at $\sqrt{s}$ =500 GeV, x_1 =0.5, x_W =0.2315 and various energy values x_Z: 1) x_Z =0.65; 2) x_Z =0.70; 3) x_Z =0.75. As can be seen from the figure, with an increase in the polar angle θ, the differential effective cross-section increases and reaches a maximum at an angle $\theta = 90°$, and with a further increase in the same angle, the effective cross-section decreases. An increase in the energy x_Z carried away by the Z^0-boson leads to an increase in the effective cross-section of the process under study.

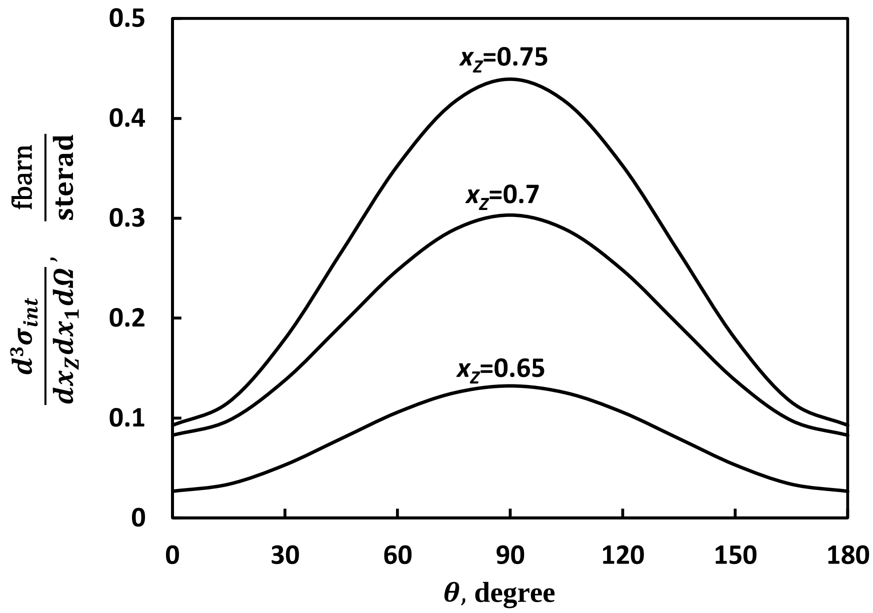

Fig. 13. Angular dependence of the process cross section $e^-e^+ \to HHZ^0$ at different energy values x_Z

Fig. 14 illustrates the dependence of the cross section of the process $e^-e^+ \to HHZ^0$ from variable x_Z at $\sqrt{s}$ =500 GeV, x_1 =0.5 and various values of the emission angle θ: 1) $\theta = 30°$; 2) $\theta = 60°$; 3) $\theta = 90°$. It can be seen from the figure that with an increase in the energy x_Z carried away by the Z^0-boson, the effective cross-section increases, an increase in the departure angle θ also leads to an increase in the effective cross-section of the process under consideration.

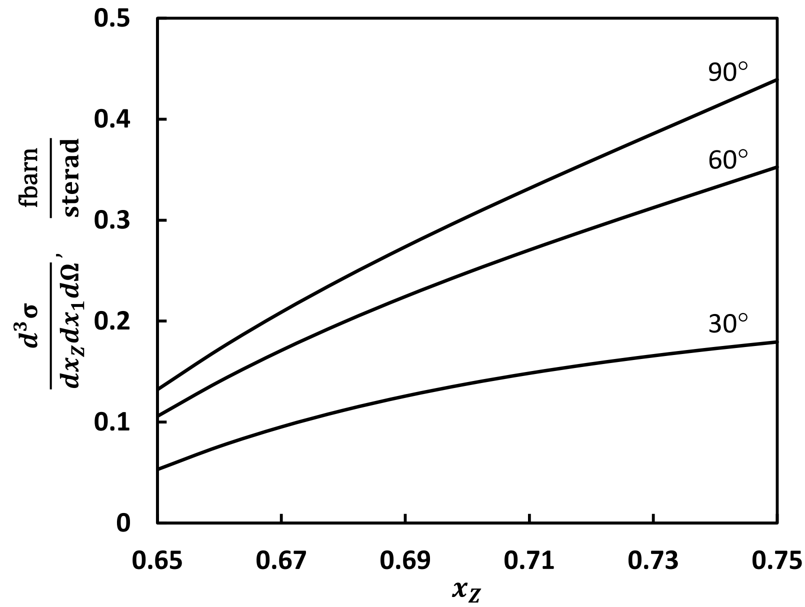

Fig. 14. Energy dependence of the cross section reaction $e^-e^+ \to HHZ^0$ at different θ

5. Conclusion

In conclusion, we note that the experimental study of the reaction of the associated production of a Higgs boson pair and a vector Z^0-boson in electron-positron annihilation is of great interest, since it allows us to measure the interaction constants of three Higgs bosons g_{HHH} and two Z^0- and two Higgs bosons g_{ZZHH}.

Although the interaction constants of vector bosons with the Higgs boson g_{ZZH} and g_{WWH} are measured in the LHC in proton-proton collisions, however, direct measurement of the interaction constants g_{HHH} and g_{ZZHH} is associated with certain difficulties. Therefore, the study of the process $e^- e^+ \to HHZ^0$ is of particular interest.

We discussed the process of the production of a vector Z^0-boson and two Higgs boson pairs in polarized electron-positron collisions $e^- e^+ \to HHZ^0$. Taking into account all possible Feynman diagrams a), b), c) and d) Fig. 1, analytical expressions for the amplitudes and differential effective cross section of the process are obtained. Left-right A_{LR} and transverse A_φ spin asymmetries due to longitudinal and transverse polarizations of the electron-positron pair are determined.The dependence of these characteristics and the differential effective cross-section on the departure angles and particle energies is studied in detail. The calculation results are illustrated with graphs.

References

Abada, A. (2013). Physics. In A. Abada, H. Baer, T. Barklow, K. Fujii, & Y. Gao (Eds.), *The International Linear Collider. Technical Design Report.* (pp. 1-204). Retrieved from https://linearcollider.org/files/images/pdf/Physics.pdf

Abdullayev, S. (2017). *The Standard Model, Properties of the Leptons and Quarks.* Baku: Zeka Print (in azerb.).

Abdullayev, S.K., Gojayev, M.Sh. (2022). Production of a higgs-boson pair in e^-e^+-collisions. *Izv. VUZov. Ser. Fizika, 64* (in Russian, *accepted for printing*).

Abdullayev, S.K. (2018). *General Properties of Fundamental Interactions.* Baku: Zeka Print (in azerb.).

Abdullayev, S.K., Gojayev, M.Sh. (2019). Associated production of a Higgs boson and heavy fermion pair in e^-e^+-collisions. *Moscow University Physics Bulletin*, *74*(1), 24-32.

Abdullayev, S.K., Gojayev, M.Sh., Saddigh, F.A. (2017). Decay channels of the Standard Higgs boson. *Moscow University Physics Bulletin*, *72*(4), 329-339.

Abdullayev, S.K., Gojayev, M.Sh., Saddih, F.A. (2015). Higgs boson decay channels: $H \to \gamma\gamma$, $H \to \gamma Z$, $H \to gg$. *Azerbaijan Journal of Physics*, *XXI*(2), 17-22.

Abdullayev, S.K., Omarova, E.Sh. (2021). Circular polarization of a g-quantum in the radiative decay $H \to f\, f\, \gamma$. *Russian Physics Journal*, *64*(2), 228-236.

ATLAS Collaboration. (2012). Observation of a new particle in the search for the Standard Model Higgs boson with the ATLAS detector at the LHC. *Physics Letters B, 716*(1), 1-29. https://doi.org/10.1016/j.physletb.2012.08.020

ATLAS Collaboration. (2018). Observation of $H \to bb$ decays and VH production with the ATLAS detector. *Physics Letters, B*, 59-86. https://doi.org/10.1016/j.physletb.2018.09.013

Barger, V., Han, T., Langacker, P., McElrath, B., & Zerwas, P. (2003). Effects of genuine dimension-six Higgs operators. *Physical Review D, 67*(11), 115001-1-13. doi:https://doi.org/10.1103/PhysRevD.67.115001

CMS Collaboration. (2012). Observation of a new boson at a mass of 125 GeV with the CMS experiment at the LHC. *Physics Letters B, 716*(1), 30-61. doi:https://doi.org/10.1016/j.physletb.2012.08.021

CMS Collaboration. (2021). Measurement of the Higgs boson production rate in association with top quarks in final states with electrons, muons, and hadrinically decaying tau leptons at s=13 TeV. *European Physical Journal C, 81*(4), 378-428.

Demirci, M. (2019). Associated production of Higgs boson with a photon at electron-positron colliders. *Physics Review, D, 100*(7), 075006(1-15). doi:https://doi.org/10.1103/PhysRevD.100.075006

Djouadi, A. (2005). *The Anatomy of Electro-Weak Symmetry Breaking. Tome I. The Higgs boson in the Standard Model.* arXiv: hep-ph/050372v2. Retrieved from https://arxiv.org/pdf/hep-ph/0503172.pdf

Djouadi, A., Kilian, W., & Mühlleitner, M. (1999). Testing Higgs self-couplings at e^+e^-- linear colliders. *European Physical Journal C, 10*(1), 27-43. doi:https://doi.org/10.1007/s100529900082

Englert, F., & Brout, R. (1964). Broken symmetry and the mass of gauge vector mesons. *Physics Review Letters, 13*, 321-323.

Glashow, S. (1967). Partial Symmetries of Weak Interactions. *Nuclear Physics, 22*, 579-588.

Gong, Y., Li, Z., Xu, X., Yang, L. L., & Zhao, X. (2017). Mixed QCD-electroweak corrections for Higgs boson production at e^+e^--colliders. *Physics Review, D, 95*(9), 093003-1-6. doi:https://doi.org/10.1103/PhysRevD.95.093003

Greco, M., Han, T., & Liu, Z. (2016). ISR effects for resonant Higgs production at future lepton colliders. *Physics Letters B, 763*, 409-415. doi:https://doi.org/10.1016/j.physletb.2016.10.078

Greco, M., Montagna, G., Nicrosini, O., Piccinini, F., & Volpi, G. (2018). ISR corrections to associated HZ production at future Higgs factories. *Physics Letters, B, 777*, 294-297. doi:https://doi.org/10.1016/j.physletb.2017.12.056

Higgs, P.W. (1964). Broken symmetries and the masses of gauge fields. *Physics Review Letters, 13*, 508-509.

Higgs, P.W. (1964). Broken symmetries massles particles and gauge fields. *Physics Letters, 12*, 132-133.

Kachanovich, A., Nierste, U., & Nišandžić, I. (2022). Higgs boson decay into a lepton pair and a photon: A roadmap to the discovery of $H \to Z\gamma$ and probes of new physics. *Physics Review, D, 105*(1), 013007(1-9).

Kazakov, D. (2014). The Higgs boson is found: what is next? *Physics-Uspekhi, 57*(9), 930-942. doi:https://doi.org/10.3367/UFNr.0184.201409j.1004

Kilian, W., Krämer, M., & Zerwas, P. (1996). Higgs-strahlung and WW fusion in e^+e^-- collisions. *Physics Letters, B, 373*(1-3), 135-140. doi:https://doi.org/10.1016/0370-2693(96)00100-1

Lanyov, A. (2014). CMS collaboration results: Higgs boson and search for new physics. *Physics Uspekhi, 57*(9), 923-930. doi:https://doi.org/10.3367/UFNr.0184.201409i.0996

Peters, K. (2017). Prospects for beyond Standard Model Higgs boson searches at future LHC runs and other machines. *Proceedings, 6th International Workshop on Prospects for Charged Higgs Discovery at Colliders* (pp. 1-6). arXiv: 1701.05124v2. doi:10.22323/1.286.0028

Rubakov, V. (2012). Large Hadron Collider's discovery of a new particle with Higgs boson properties. *Physics-Uspekhi, 55*(10), 949-957. doi:https://doi.org/10.3367/UFNr.0182.201210a.1017

Salam, A. (1968). Weak and electromagnetic interactions, in elementary particle physics: relativistic groups and analicity. In N. Svartholm (Ed.), *Proceedings of the eighth Nobel symposium* (p. 367). Almquvist and Wiksell.

Shiltsev, V. (2012). High-energy particle colliders: the past 20 years, the next 20 years, and the distant future. *Physics-Uspekhi, 55*(10), 965-976. doi:https://doi.org/10.3367/UFNr.0182.201210d.1033

Weinberg, S. (1967). A Model of leptons. *Physics Review Letters, 19*, 1264-1266.